ELSEVIER

Journal of Photochemistry and Photobiology A: Chemistry 110 (1997) 257–266

Journal of PHOTOCHEMISTRY AND PHOTOBIOLOGY A: CHEMISTRY

Solvatochromic effects in the absorption and fluorescence spectra of indazole and its amino derivatives

Subit K. Saha, Sneh K. Dogra *

Department of Chemistry, Indian Institute of Technology Kanpur, Kanpur 208016, India

Received 7 February 1997; received in revised form 14 May 1997; accepted 2 June 1997

Abstract

Absorption and fluorescence spectra of Indazole (In) in five solvents and those of 5-amino, 6-amino, and 7-aminoindazoles (5-AI 6-AI, 7-AI) in thirteen solvents have been studied. Using the multiparametric approach of Taft et al., spectral characteristics of these molecules have been analysed on the basis of electrostatic effects, hydrogen bond donor ability and hydrogen bond accepting ability of the solvents. In the excited singlet state, all three effects are nearly equally prominent, whereas in the ground state 5-AI acts as a better hydrogen bond acceptor than the other amines. Stokes shifts and the difference between the radiative decay constants determined experimentally and using Strickler and Berg's equation indicate different geometries of the amines in the S_0 and S_1 states. A decrease in the non-radiative decay constants of 5-AI and 6-AI with an increase in the polarity of the solvents predict better planar geometry in the S_1 state in comparison to that in the S_0 state. Semi-empirical quantum mechanical calculations have been used to find the nature of transitions, total atomic charges at the basic centres and dipole moments of all the aromatic amines in the S_0 and S_1 states. Results so obtained are compared and discussed.

Keywords: Absorption spectra of indazole; Fluorescence spectra; Ground and excited state

1. Introduction

Three characteristics of fluorescence spectroscopy have been widely used to explore the fundamental phenomena of photophysics [1,2], properties of macro and biologically active molecules [3–5], and the utility of the fluorophore as a photosensitizer [6]. These are solvatochromism [1,7–9], fluorescence quenching [1,10], and the energy transfer process [6]. The solvatochromic effect has been widely used to find the nature and the polarity at the various sites of biologically active molecules besides determining the change in dipole moment on excitation and the nature of interactions between the fluorophore and environments.

In the last few years, our main emphasis has been to study the effect of solvents of different polarity [11–13] and acid/base concentrations on the spectral characteristics of different fluorophores so that they can be used as probe molecules. The present study describes the effect of different kinds of solvents on the spectral properties of In, 5-AI, 6-AI, and 7-AI. Various polarity scales have been used to calculate the excited state dipole moments. Semi-empirical quantum mechanical calculations were carried out on these molecules to find out the dipole moments, nature of transitions, and the total atomic charges at the basic centres in the S_0 and S_1 states. Change in dipole moments upon excitation, calculated theoretically and experimentally, are compared and discussed.

2. Materials and methods

In, 5-AI, and 6-AI were procured from Aldrich Chemical company UK, whereas 7-AI was obtained from K&K Laboratories. Each compound was further purified as described earlier [14–17]. Cyclohexane (SD Fine), dioxane, acetonitrile, and methanol (E. Merck) and ether (Allembic) were further purified as described in the literature [18]. All other solvents were either of AnalR grade or spectroscopic grade and thus were used as received. Triply distilled water was used for aqueous solutions.

The absorption spectra were recorded on a Shimadzu spectrophotometer model UV 190, equipped with chart recorder model U135. Fluorescence spectra were recorded on a scanning spectrofluorometer fabricated in our laboratory, details of which are available elsewhere [19]. The concentrations of the test solutions were 2×10^{-5} M. Spectral measurements

* Corresponding author.

1010-6030/97/$17.00
PII S1010-6030(97)00192-5

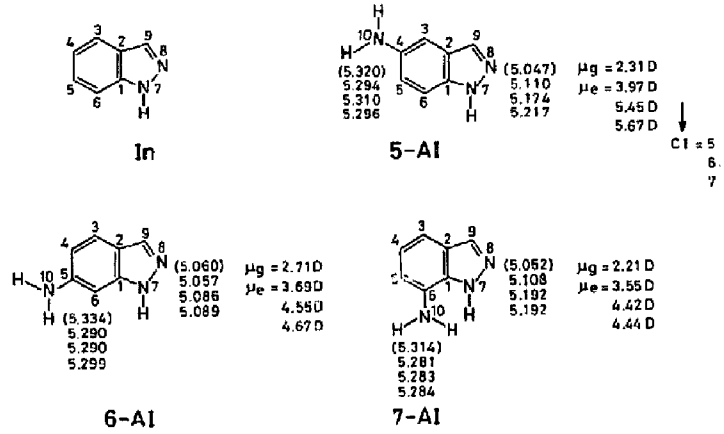

Fig. 1. Charge densities in the ground and excited singlet state (parenthesis) at each atom.

were made immediately after the preparation of the solutions. Fluorescence spectra were corrected according to the method of Parker [20]. Fluorescence quantum yields were determined with solutions having absorbance less than 0.1 and using quinine sulphate in 0.1 N H_2SO_4 as a reference [21] ($\phi_{fl} = 0.55$). Excited state lifetimes were measured on a time-correlated single photon counting nanosecond spectrofluorometer, supplied by Applied Photophysics Limited. Details are available in our recent paper [22].

The pcmodel 2 program [23] was used to find the starting geometry of each molecule. This program enables us to draw the structure, optimize roughly the geometry using the MM2 force field and generate the corresponding coordinates. The ground state geometries of all the molecules were then optimized using the AM1 method [24] (mopac, QCPE program No. 455, version 4.0) on a HP 9000/750, Super mini computer using the above-mentioned coordinates. The ground state dipole moment (μ_g), total energy and charge densities at each basic atom have been calculated. The transition energy ΔE_{i-j}, corresponding to the excitation of an electron from the orbital ϕ_i (occupied in the ground state) to ϕ_j (unoccupied in the ground state) have been calculated using CNDO/S-CI calculations [25]. The excited state geometries of all the amines were also optimized using AM1 method by taking into account the configuration interaction calculations on 100, 400 and 1225 configurations (CI = 5, 6 and 7 in MOPAC). The geometries of all the amines were fully optimized for CI = 5 and 6, whereas, for CI = 7, only 5-AI was satisfying all the tests. As there is not much difference between the results obtained using CI = 6 and CI = 7 for 5-AI, we assumed that the results obtained for 6-AI and 7-AI will not be far from the true values, even though these molecules are not fully optimized for CI = 7. The total atomic charges at each basic centres and the dipole moments in S_0 and S_1 states are compiled in Fig. 1 and the data show that there are not many differences between the results obtained for CI = 6 and CI = 7.

3. Results and discussion

3.1. Absorption spectrum

The experimental (recorded in cyclohexane) and calculated transition wavelengths of different molecules along with oscillator strengths are compiled in Table 1. Agreeing with earlier results [14], the first two absorption bands of In are nicely structured in all solvents, with the vibrational frequencies of $770 \pm 20\ cm^{-1}$ for the first band and $1100 \pm 50\ cm^{-1}$ for the second band respectively. On the other hand, the absorption spectra of 5-AI and 7-AI are structureless and broad, whereas that of 6-AI is broad in comparison to In but possesses some structure in comparison to 5-AI and 7-AI.

All the transitions predicted by theory are $\pi \rightarrow \pi^*$ in nature. This is supported by the large values of the extinction coefficients ($> 10^3\ mol^{-1}\ l\ cm^{-1}$) and fluorescence quantum yield. The results agree with the values reported on indazole moiety [26]. The agreement between the experimental and theoretical values are quite good (maximum discrepancy is of $\sim 1000\ cm^{-1}$, except in the third band of 6-AI where it is

Table 1
Absorption band maxima (λ_{ab}) in cyclohexane and calculated by CNDO/S-CI method and the oscillator strengths of In, 5-AI, 6-AI, and 7-AI

Molecule	λ_{ab} (nm)		Oscillator Strength
	Expti	Theor	
Indazole	294	296	0.011
	256	254	0.091
5-Aminoindazole	326	313	0.031
	254	257	0.015
6-Aminoindazole	296	305	0.012
	274	275	0.026
	235	266	0.162
7-Aminoindazole	296	306	0.018
	256	257	0.093

Table 2
Contribution of various molecular orbitals in the longest wavelength singlet transition and their localization

Compound	Transition (nm)	Configuration	Composition (%)	MO	Localization
Indazole	296	21→23	49	21π	1,2,4,5,8
		22→24	36	22π	3,5,6,7,8,9
				23π*	2,5,6,8,9
				24π*	1,3,4,6
5-AI	313	25→26	64	24π	2,3,5,6,7,8,9
		24→27	25	25π	1,3,4,6,7,10
				26π*	2,3,5,6,8,9
				27π*	1,3,4,6
6-AI	306	24→26	40	24π	1,3,4,6,7,9
		25→26	8	25π	2,5,6,8,10
		25→27	45	26π*	2,3,5,6,8,9
				27π*	1,3,4,6
7-AI	307	24→26	27	24π	1,2,4,5,8
		24→27	10	25π	3,5,6,7,9,10
		25→26	30	26π*	2,3,5,6,8,9
		25→27	28	27π*	1,3,4,6

1620 cm^{-1}), considering the approximations used in these calculations. The major contributions of various molecular orbitals involved in the longest wavelength singlet transition and their localization at various centres are listed in Table 2. It can be seen from the data of Table 2 that in all the molecules, configuration interactions involved in the long wavelength transition are from the transitions involving two HOMOs and two LUMOs. In all the molecules, the first LUMO is quite a bit delocalized over the pyrazole ring as well, whereas the second LUMO is localized only on the benzene ring. On the other hand, the first HOMO in In and 7-AI, and the second HOMO of 5-AI involve atomic centres present in the pyrazole ring, whereas the other HOMO is mostly localized over the benzene ring. The participation of the configuration interaction involving the HOMO (localized either on hetero ring or delocalized over the complete molecule) and LUMO (localized over the benzene ring) is minimum in the longest wavelength transition of 5-AI. In other words, charge migration from the amino group to the aromatic moiety is a maximum in 5-AI. This is supported by the fact that the decrease in the total atomic charge on the amino nitrogen and the increase in the total atomic charge on the $\geq N$ is a maximum in the case of 5-AI in comparison to other molecules (Fig. 1). This may be one of the causes of the maximum red shift observed in the absorption spectrum of In in 5-AI, in comparison to other amines.

The other point to be considered is the presence of vibrational structure in the absorption spectrum of 6-AI in comparison to either 5-AI or 7-AI. This could be due to either less participation of lone pair (1) with the π-cloud of In or to the presence of some rigidity in the amino nitrogen–carbon bond. The latter seems to be more feasible because the bond order calculated between the amino nitrogen and the carbon atom connecting the amino group is larger for 6-AI (1.098) in comparison to those in 5-AI (1.075) and 7-AI (1.069).

3.2. Fluorescence spectrum

The fluorescence spectrum of In [14] is nicely structured in all the solvents and, as expected, a mirror image symmetry is observed with the absorption spectrum, indicating that the geometry of In in the emitting and absorbing states is the same. On the other hand, fluorescence spectra of all the amines are broad and structureless. Contrary to the absorption spectra, the fluorescence spectra are more sensitive to the nature of the solvents. This is consistent with the fact that greater charge transfer takes place from amino group to the aromatic ring in the S_1 state in comparison to the ground state. A continuous red shift observed in the fluorescence spectra of all the amines with an increase in the polarity of the solvents indicates the increase in the delocalization of the lone pair of electrons of the amino group throughout the aromatic ring in the S_1 state. The common features observed in the fluorescence spectra of all the amines are as follows. (i) The fluorescence excitation spectra recorded at the band maximum and two other wavelengths (red shifted to the band maximum) are exactly similar to each other and to the respective absorption spectra indicating that there is only one conformer for each molecule in S_0 state. (ii) There is a lack of mirror image symmetry between the modified absorption and fluorescence spectra, indicating a change in the geometry between the electronic ground state of these molecules and their first excited singlet states. Such a plot, as a representative one (using the method suggested by Birk's and Dyson [27]), is shown in Fig. 2 for 7-AI in water. (iii) The Stokes shifts observed for 5-AI, 6-AI, and 7-AI in cyclohexane are 3520, 3890, and 4570 cm^{-1} respectively, which are quite large. Since the molecular volumes of these molecules are nearly similar, the large Stokes shifts observed in the same solvent are a good indication of the increase in the dipole moment of these molecules on excitation.

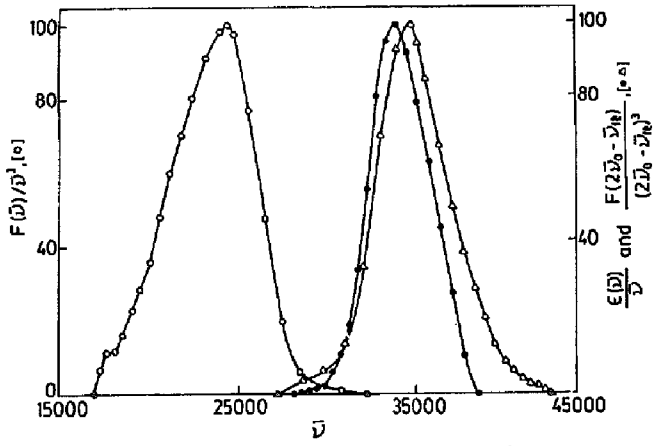

Fig. 2. 253Modified absorption spectrum [$\epsilon(\bar{\nu})/\bar{\nu}$, O-O-O]. Modified fluorescence spectrum [$F(\bar{\nu})/\bar{\nu}^3$, Δ-Δ-Δ] and its reflection [$F(2\bar{\nu}_0-\bar{\nu})(2\bar{\nu}_0-\bar{\nu})^3$, ×-×-×] for 7-AI in water.

Fluorescence quantum yields and the lifetime data of the three molecules are compiled in Table 3. The values of k_r and k_{nr}, calculated using the following relations, are also compiled in Table 3. The values of theoretical or natural radiative lifetime

$$k_r=\phi_{fl}/\tau_f,\quad k_{nr}=1/\tau_i-k_r$$

$\tau_{FM}{}^i$ (characterising the ground state geometry and the transition moment in the absorption process) in some solvents was calculated using the Strickler and Berg equation [28] and the radiative lifetimes $\tau_{FM}{}^e$ (indicative of the relaxed excited singlet state geometry and the transition moment involving the spontaneous fluorescence emission process) are listed in Table 3. Behaviour of these parameters for each amine is different in different solvents. The ϕ_{fl} and τ_f increase with the increase in the polarity and hydrogen bonding capacity of the solvents in the case of 5-AI, nearly remain constant

Table 3
Fluorescence quantum yield (ϕ_{fl}), singlet state lifetime (τ_f, ns), radiative ($k_r\times10^{-7}\ s^{-1}$) and non-radiative decay constants ($k_{nr}\times10^{-7}\ s^{-1}$), $k_{FM}{}^e$ and $k_{FM}{}^i$ indifferent solvents

Solvent	ϕ_{fl}	τ_f	k_r	k_{nr}	$k_{FM}{}^e$	$k_{FM}{}^i$
5-AI						
Cyclohexane	0.14	4.9	2.9	17.5	–	–
Acetonitrile	0.18	4.7	3.8	16.6	–	–
Methanol	0.37	6.4	5.8	9.8	5.8	3.5
Water	0.57	12.5	4.6	3.4	–	–
6-AI						
Cyclohexane	0.34	4.0	8.5	16.5	–	–
Acetonitrile	0.33	5.4	6.1	12.4	–	–
Methanol	0.31	3.1	10.0	22.5	10.0	8.9
Water	0.39	4.4	8.9	13.9	–	–
7-AI						
Acetonitrile	0.30	4.63	6.48	15.1	6.5	8.0
Methanol	0.11	1.69	6.5	52.7	5.5	6.0
Water	0.07	1.74	3.85	53.6	3.85	4.0

for 6-AI and decrease under the similar environments for 7-AI. The values of $\tau_{FM}{}^e$ are less than $\tau_{FM}{}^i$ for 5-AI and 6-AI in methanol, whereas they are greater in the case of 7-AI. It is known that the flexible molecules in the excited states increase the non-radiative decay rate constants of these states [29]. Data of Table 4 and the discussion revealed in Section 3.3 clearly indicate that the hydrogen bonding (proton donor capacity of amino group and proton accepting nature of the ≥N atom) in the excited state is much stronger than that in the ground state. This will contribute to the stabilization of a much more planar geometry of these amines (especially for 5-AI and 6-AI, where the location of the proton donor amino group and proton acceptor ≥N moiety is favourable) and thus will decrease the non-radiative decay rate. The results observed in the case of 5-AI are consistent with the above explanation. A relatively small decrease in k_{nr} for 6-AI in comparison to 5-AI could be due to the fact that in 6-AI, as stated earlier (Section 3.1), the bond order between amino nitrogen and carbon of the indazole is greater than that in 5-AI. So the contribution to the stabilization by the change in the geometry of this amine on excitation may be small in the S_1 state. The change in the geometry of these amines in the S_1 state is further supplemented by the fact that $k_{FM}{}^e$ exceeds $k_{FM}{}^i$ in both 5-AI and 6-AI. A similar increase in $k_{FM}{}^e$ compared with $k_{FM}{}^i$ has also been observed in 2-aminonaphthalene [30] by El-Bayoumi et al. and in some antioxidants by Sow and Durocher [31]. Both the groups have explained their results on the basis that geometry changes do occur in these molecules upon excitation. For example, Mataga [32] suggested a structural change of the amino group from the essentially sp^3 configuration in the ground state to sp^2 configuration in the S_1 state, whereas in the case of antioxidants a more planar excited state has been proposed and confirmed. In agreement with Meach et al. [33] we also propose that the intramolecular structural reorganisation and the solvent–solute, dipole–dipole reorientation of the polar and/or protic

Table 4
Coefficients of the relevant solvent parameters as defined by Eq. (1) and E^0 for different molecules

Molecules	E^0 (10^4 cm^{-1})	c (10^2 cm^{-1})	a (10^2 cm^{-1})	b (10^2 cm^{-1})	
Absorption Data					
Indazole	3.485	−6.129	3.225	−2.52	(0.93)
5-Aminoindazole	3.053	−4.215	11.57	−0.799	(0.98)
6-Aminoindazole	3.382	−5.058	6.014	−4.997	(0.85)
7-Aminoindazole	3.379	−3.11	1.59	−4.767	(0.77)
Fluorescence Data					
Indazole	3.378	−0.684	−3.266	−5.71	(0.99)
5-Aminoindazole	2.697	−7.854	−9.106	−11.81	(0.98)
6-Aminoindazole	2.978	−14.91	−7.416	−10.65	(0.98)
7-Aminoindazole	2.917	−16.75	−21.10	−11.22	(0.99)

Values in parentheses give regression coefficients.

solvents play a major role on the photophysical parameters of these molecules.

The behaviour of 7-AI is very different from the other two amines. In this case, the fluorescence quantum yield and the lifetime decrease with the increase in the polarity and hydrogen bonding solvents. There could be some uncertainty in the lifetimes in methanol and water because of the lower limits of the instrument. Data of Table 3 indicate that the value of k_{nr} increases with an increase of solvent polarity and the values of $k_{FM}{}^e$ are less than those of $k_{FM}{}^t$ in all the solvents. This could be, as said earlier, due to the larger change in the intramolecular structural reorganisation of the substituent on excitation, which leads to larger Stokes shifts in comparison to other amines. This may also explain the quenching of the fluorescence in solvents of higher polarity and hydrogen bonding due to greater interaction. Similar results have been observed in the case of 6-hydroxy-1-ethyl-5,7,8-trimethyl-1,2,3,4-tetrahydroquinoline [31] and by Mataga and Kuboto [32].

3.3. Solvatochromism

The absorption band maxima ($\bar{\nu}_{ab}$) and fluorescence band maxima ($\bar{\nu}_{fl}$) of In, 5-AI, 6-AI, and 7-AI in different solvents, along with their refractive indices and dielectric constants are compiled in Table 5. The solvents have been arranged as polar/aprotic, polar/protic and chlorinated methanes. Fluorescence intensity is quite small in chlorinated solvents and the intensity decreases with an increase in the number of chlorine atoms, non-fluorescent in carbon tetrachloride, in agreement with the fact that chlorinated solvents are good fluorescence quenchers [35,36]. BK and BK′ parameters for different solvents have been calculated using Eqs. (6) and (7), taking $\alpha = 0$ (when the molecule is not polarized) and $2\alpha/4\pi\epsilon_0 \cdot a^3 = 1$ when the molecule has isotropic polarizability.

Few empirical and theoretical solvent polarity scales are in use to explore the solvatochromic effects [37–41]. However, the disadvantages of such scales, e.g. the Z parameters

Table 5
Spectroscopic parameters of In, 5-AI, 6-AI, and 7-AI in different solvents

Solvent	Indazole				5-AI		6-AI		7-AI	
	n	ϵ	$\bar{\nu}_{ab}$	$\bar{\nu}_{fl}$	$\bar{\nu}_{ab}$	$\bar{\nu}_{fl}$	$\bar{\nu}_{ab}$	$\bar{\nu}_{fl}$	$\bar{\nu}_{ab}$	$\bar{\nu}_{fl}$
Cyclohexane	1.424	2.02	34 080	33 780	30 620	27 100	33 830	29 940	33 807	29 240
n-Hexane	1.372	1.88			30 560	26 950	34 060	30 120	33 830	29 240
n-Heptane	1.387	1.92			30 560	27 030	33 850	29 500	33 920	
Dioxane	1.439	2.21			30 190	26 040	33 000	28 900	33 470	27 850
Ether	1.352	4.34			30 300	25 970	33 310	28 570	33 560	28 010
Ethylacetate	1.370	6.02			30 360	26 110	33 330	28 650	33 470	27 780
Acetonitrile	1.344	37.5	34 020	33 560	30 380	25 710	33 580	28 170	33 540	27 170
Methanol	1.331	32.6	33 960	33 450	31 250	25 000	33 670	27 550	33 560	25 770
Ethanol	1.359	24.55			31 210	25 060	33 630	27 620	33 270	26 040
n-Propanol	1.384	20.33			31 230	24 880	33 690	27 620	33 250	25 320
Water	1.333	80.2	33 960	33 330	31 430	24 630	34 040	26 950	33 780	24 450
CH_2Cl_2		1.33			30 640	26 390	33 530	28 450	33 420	27 320
Chloroform	1.444	4.73			30 680	26 040	–	–		

of Kosower [42] and the Reichardt–Dimroth [34] parameter $E_T(30)$, are that information is lost about the individual contribution of different solvent effects. To over come this, Taft et al. [43,44], have proposed the solvatochromic effect comparison method (SCM); this is a multiparameter approach which separates the effects of general solvent polarity (π), hydrogen bond donor ability (α) and hydrogen bond acceptor ability (β) of the solvents on the spectral properties. The equation describing these effects is:

$$E = E^0 + c\pi + a\alpha + b\beta \quad (1)$$

where a, b, and c are the coefficients and E^0 is the spectral maxima independent of solvent effects. The values of these coefficients and E^0 of all the molecules are compiled in Table 4. The regression coefficients obtained for the fluorescence data are very good (~0.98), but the values of regression coefficients obtained for the absorption data of 6-AI (0.59) and 7-AI (0.77) are not good. This value for 6-AI improved when we neglected the data recorded in dioxane as solvent (0.85). This deviation in dioxane is consistent with the fact that dioxane behaves as a pseudopolar solvent of variable polarity function, which depends upon the solute's electric field, as a result of conformation polarizability [45]. In our case, μ_g is maximum for 6-AI, creating a larger electrical field around dioxane solvent molecules. On the other hand, the value of the regression coefficient for 7-AI improved (0.97) when the data recorded in chloroform and methylene chloride were neglected. This could be due to some other kind of interaction, also present in other amines [11].

The signs of coefficients b and c are negative for both absorption and fluorescence spectra, indicating the stabilization of the ground and excited states. The sign of a is positive and negative for the absorption and fluorescence data respectively. This is consistent with the fact that the amino group acts as a proton acceptor in the ground state, hinders the participation of a lone pair of electrons with the π-cloud of the ring and thus causes a blue shift in the absorption spectrum, whereas in the S_1 state the amino group acts as a proton donor because of the participation of a lone pair with the π-cloud of the ring and thus stabilizes the excited state. This is consistent with the decrease in atomic charge at the amino nitrogen on excitation (Fig. 1). In the ground state, the dipole–dipole contribution is consistent with the trend observed in the μ_g, i.e. $\mu_g(7\text{-AI}) < \mu_g(5\text{-AI}) < \mu_g(6\text{-AI})$, whereas in the S_1 state the trend observed in the dipole–dipole interactions is also consistent with the Stokes shifts observed in these amines in any given solvent. 5-AI acts as a poor hydrogen bond donor in the S_0 state in comparison to other molecules, but as a better hydrogen bond acceptor, consistent with the atomic charges at the amino nitrogen atom and ≥N moiety (Fig. 1). On the other hand, 6-AI and 7-AI act as a better proton donor in the S_0 state and agrees with the presence of a resonance structure (Scheme 1) in 6-AI and steric hindrance from the >NH proton in the pyrazole ring. Data of Table 4 further show that in the S_1 state all the molecules act as proton donor and proton acceptor moieties. This is consistent with the earlier results [15–17] that all these amines show biprotonic phototautomerism. In the S_1 state, the $-NH_2$ group becomes a strong acid and acts as a proton donor, whereas ≥N atom becomes a strong base and acts as a proton acceptor.

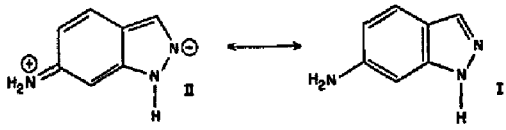

Scheme 1.

3.4. Dipole moments in the ground state

The values of μ_g calculated for all the molecules using the mopac program are compiled in Table 6. In our earlier study [46] it is found that the agreement between theoretical (0.45 D) and the experimental [47] (0.5 D in benzene) value of μ_g for quinoxaline is not bad. Similarly we hope that the calculated value of μ_g for these molecules will not be far off the actual values.

Data of Table 6 indicate that μ_g increases with the addition of an amino group to the indazole molecule. The increase in μ_g is in the order of 7-AI, 5-AI and 6-AI. It is well established that the bond moments of the individual group contributes maximum to the total dipole moment of the molecule. The small differences in the μ_g of the aminoindazoles are due to the different directions of the bond moment of the amino group substituted at different positions of the indazole moiety with respect to that of indazole. Although the contributions to the total dipole moment from the mesomeric structures is very small, its effect seems to be greater in 6-AI as compared to that in 5-AI and 7-AI. This is because of the resonance structures present in 6-AI, but absent in 5-AI and 7-AI. This is supported by: (i) the ground state total atomic charges at the amino nitrogen atom and ≥N atom of the three amines, (ii) the first oxidation potential [48] (which is due to the ejection of electron from the amino group) of 6-AI (0.87 V), 7-AI (0.734 V) and 5-AI (0.71 V), and (iii) the pK_a value

Table 6
Dipole moments in the S_0, S_1 and S_2 states and Onsager cavity radius for In, 5-AI, 6-AI and 7-AI

Molecule	$a \times 10^{10}$ (m)	μ_g (D)	μ_e (D)			
			BK		BK′	
			$\alpha=0$	$\alpha=1$	$\alpha=0$	$\alpha=1$
In	3.09	1.62	2.96	2.44	–	–
5-AI	3.42	2.31	5.92	4.50	5.10	3.49
6-AI	3.51	2.71	7.05	5.34	6.74	4.49
7-AI	3.32	2.21	6.87	5.01	6.18	4.05

BK and BK′ represents the values of μ_e in the S_1 state determined from Figs. 4–7.

of the protonation reaction of amino group 6-AI [16] (3.9), 7-AI [17] (3.9) and 5-AI [15] (5.27).

3.5. Dipole moments in the excited state

Oshika [49], Lippert [50,51] and Mataga et al. [52] were the first to derive equations relating changes in the dipole moments on excitation with spectral changes. These equations were modified by Liptay [53], Bilot and Kawaksi [54] and Bhakhshiev [55] by including polarizability of the fluorophores and dispersive interactions. We will be using BK and BK′ equations to calculate the excited state dipole moments.

For a spherical molecule, and taking into account the polarizability (α) of the fluorophores, the general equations can be written as [8]:

$$\bar{\nu}_{ab}-\bar{\nu}_{fl}=m_1 f(D,n)+\text{const} \tag{2}$$

$$\bar{\nu}_{ab}+\bar{\nu}_{fl}=-m_2[f(D,n)+2g(n)]+\text{const} \tag{3}$$

where

$$m_1=\frac{(\mu_e-\mu_g)^2}{\beta a^3} \tag{4}$$

$$m_2=\frac{\mu_e^2-\mu_g^2}{\beta a^3} \tag{5}$$

$$f(D,n,\alpha/a^3) \tag{6}$$
$$=\frac{\dfrac{D-1}{2D+1}-\dfrac{n^2-1}{2n^2+1}}{\left(1-\dfrac{1}{4\pi\epsilon_0}\dfrac{2\alpha}{a^3}\dfrac{D-1}{2D+1}\right)\left(1-\dfrac{1}{4\pi\epsilon_0}\dfrac{2\alpha}{a^3}\dfrac{n^2-1}{2n^2+1}\right)^2}$$

$$g(n,\alpha/a^3)=\frac{\dfrac{n^2-1}{2n^2+1}\left(1-\dfrac{1}{4\pi\epsilon_0}\dfrac{\alpha}{a^3}\dfrac{n^2-1}{2n^2+1}\right)}{\left(1-\dfrac{1}{4\pi\epsilon_0}\dfrac{2\alpha}{a^3}\dfrac{n^2-1}{2n^2+1}\right)^2} \tag{7}$$

where $\beta=2\pi\epsilon_0 hc=1.1051\times10^{-35}\,C^2$. In the case of isotropic polarizability of molecules, the condition of $2\alpha/(a^3 4\pi\epsilon_0)=1$ is frequently satisfied and Eq. (2) will represent the BK equation. If the polarizability of the molecule is neglected, Eq. (2) reduces to Eq. (8), derived by Lippert [51] and Mataga et al. [52],

$$\bar{\nu}_{ab}-\bar{\nu}_{fl}=m_1\left(\frac{D-1}{2D+1}-\frac{n^2-1}{2n^2+1}\right)+\text{const} \tag{8}$$

Fig. 3 shows the plot of Stokes shifts versus $E_T(30)$ parameters. As mentioned earlier, this scale accounts for both general and hydrogen bonding interactions; a good correlation is observed except for dioxane, which has been explained earlier. Unlike other aromatic amines [11], the solvatochromic effect observed for these molecules, except for 7-AI, in chloromethanes (wherever the fluorophores are fluorescent) fits nicely in this plot indicating that other kinds of specific interaction between the fluorophore and chlorinated solvents are nearly absent.

Figs. 4 and 5 present the plots between Stokes shifts versus BK parameters when $\alpha=0$ and $\alpha=1$, whereas Figs. 6 and 7 depict plots between ($\bar{\nu}_{ab}+\bar{\nu}_{fl}$) versus BK′ parameters when $\alpha=0$ and $\alpha=1$ respectively. It is clear from Figs. 4 and 5 that Stokes shifts observed in polar/protic solvents are much larger than expected from the linear relations. The large deviation from linearity shown by the protic solvents is due to the fact that the hydrogen bond between the protic solvents and the lone pair of the amino group in the S_0 state is broken on excitation and the hydrogen bond is formed between the

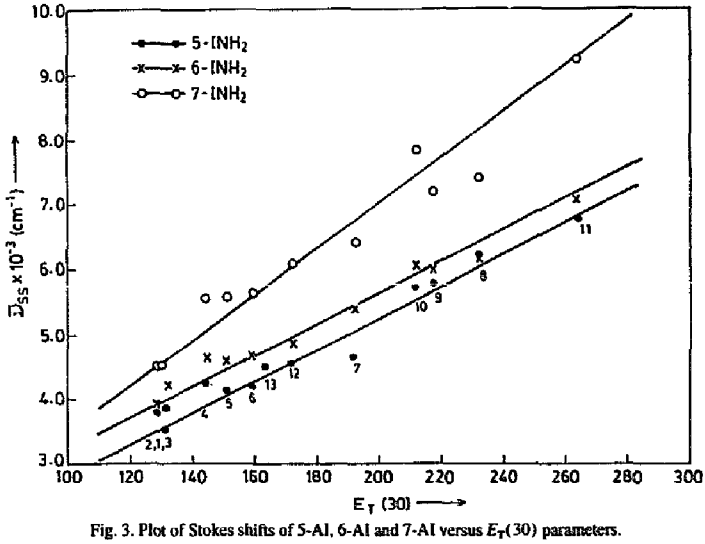

Fig. 3. Plot of Stokes shifts of 5-AI, 6-AI and 7-AI versus $E_T(30)$ parameters.

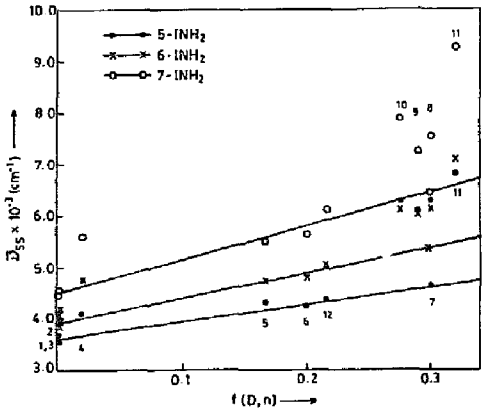

Fig. 4. Plot of Stokes shifts of 5-AI, 6-AI and 7-AI in different solvents versus BK parameters when $\alpha = 0$.

amino proton and the lone pair of the solvent molecules. As a result, a large anomalous bathochromic shift is observed in the fluorescence spectra of these amino compounds. This is reflected by the positive values of the coefficients a in absorption spectra and the negative values in the fluorescence spectra. As explained earlier, besides this, the $\geq$N moiety also acts as a proton accepting centre which causes a further red shift and is substantiated by the atomic charges which decrease and increase at the amino and $\geq$N nitrogen atom, respectively, of each amine on excitation. If the hydroxylic solvents are omitted, the regression coefficients observed for BK ($\alpha = 0$) and ($\alpha = 1$) parameters are found to be 0.98 ± 0.01 and 0.96 ± 0.01 respectively, whereas the values of regression coefficients observed from the plots of Figs. 6 and 7 are 0.96 ± 0.02 when $\alpha = 0$ and 0.93 ± 0.02 when $\alpha = 1$. Although correlation coefficients increase to unity when α decreases from 1 to 0, no clear conclusion can be drawn from our results whether or not polarizability plays any role in finding the excited state dipole moments.

The μ_e for each molecule is determined from the slope of the linear part of the plots of Figs. 4–7 and using μ_g and Onsager's cavity radius obtained theoretically. The Onsager cavity radius is taken as half the maximum distance between any two atoms present in the molecule, after its geometry being optimized and is listed in Table 6. The values of a have also been calculated using the method of Prabhumirshi et al. [56] and the values are found to be 3.39, 3.47 and 3.35 Å for 5-AI, 6-AI and 7-AI respectively. As expected the agreement between these values are quite good, thus we have used the earlier data. This indicates that cavity radii of the three amines are not very different from each other, as expected from their structures. The results indicate that μ_e is a function of polarizability of the fluorophore and in any method μ_e obtained with $\alpha = 0$ is always greater than those obtained by taking $\alpha = 1$. We have tried to solve this problem by doing semi-empirical quantum mechanical calculations, by taking into account configuration interactions. Similar to the experimental results, theory also predicts $\mu_e > \mu_g$, and also indicates that the result obtained by taking CI = 6 and CI = 7 are nearly equal. The theoretical results show that for 6-AI and 7-AI better agreement is achieved with the experiment if BK′ parameters are used and the polarizability is playing a major role in the μ_e, whereas in the case of 5-AI the BK parameters give better agreement in μ_e. This could be due to the fact that the changes observed in the charge densities at the amino nitrogen and $\geq$N are a maximum in 5AI.

4. Conclusions

The agreement between the absorption band maxima observed experimentally and theoretically is very good.

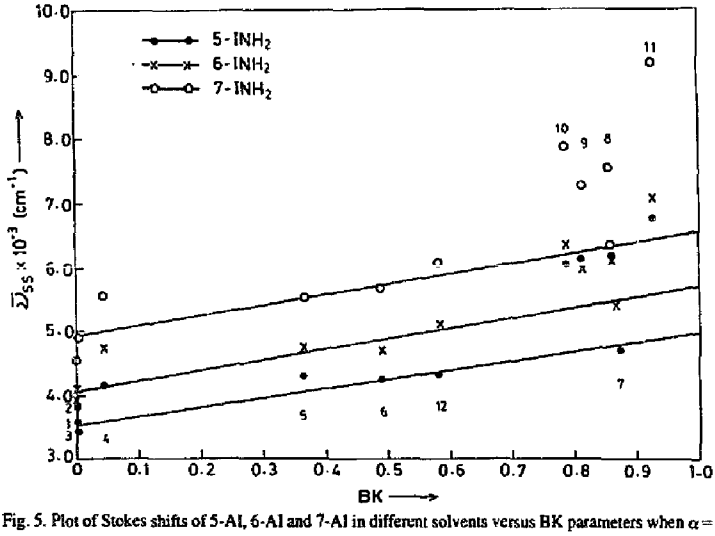

Fig. 5. Plot of Stokes shifts of 5-AI, 6-AI and 7-AI in different solvents versus BK parameters when $\alpha = 1$.

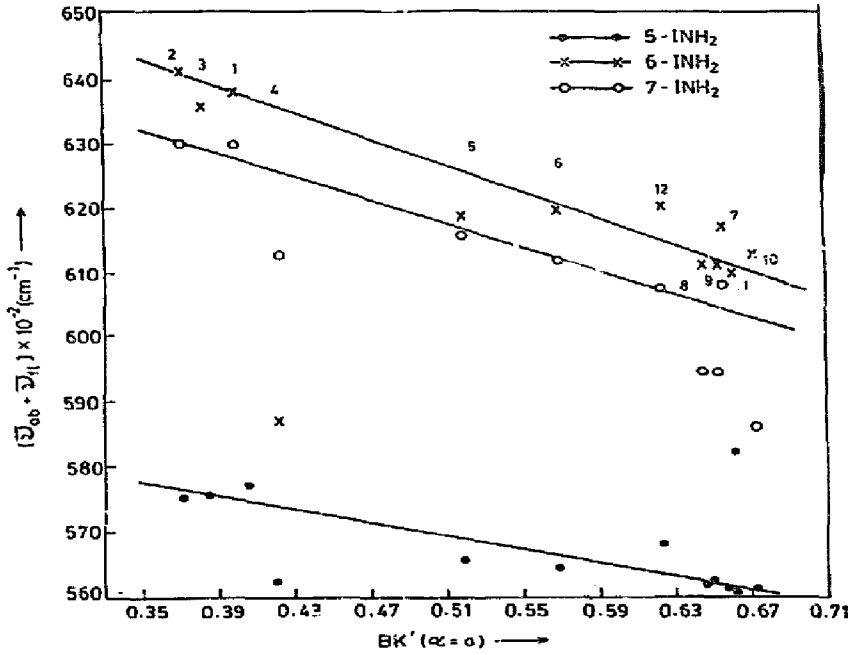

Fig. 6. Plot of $\bar{\nu}_{ab} + \bar{\nu}_{fl}$ of 5-AI, 6-AI and 7-AI in different solvents versus BK′ parameters when $\alpha = 0$.

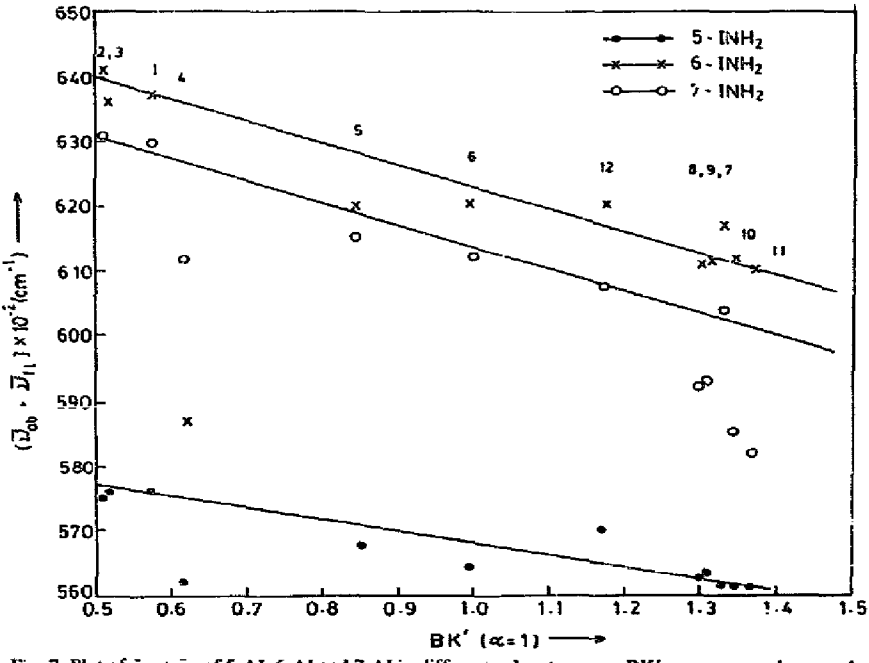

Fig. 7. Plot of $\bar{\nu}_{ab} + \bar{\nu}_{fl}$ of 5-AI, 6-AI and 7-AI in different solvents versus BK′ parameters when $\alpha = 1$.

Ground state dipole moments, calculated using the mopac program, indicate that charge transfer from the amino group to the heterocyclic ring is a maximum in 6-AI. The absorption and fluorescence spectra in different solvents have indicated that these amines act as proton acceptor in the S_0 state and proton donor in the S_1 state. Fluorescence excitation spectra recorded at the band maxima and at wavelengths towards the red side of the band maxima indicate that only one conformer is present in the S_0 state. Similarly, fluorescence spectra obtained when excited at different wavelengths show that the emission occurs from the most relaxed state. Comparison of the modified absorption and the fluorescence spectra and the radiative fluorescence decay rate, calculated using Strickler and Berg equation and determined experimentally, show a lack of mirror image symmetry, which reflects different nuclear configurations in the S_n and S_1 states. A decrease in the non-radiative decay constants of 5-AI and 6-AI with an increase in the polarity of the solvents reflects the stabilization of the planar geometry of these amines in the S_1 state. On the other hand, the increase in the non-radiative decay constant for 7-AI under the above environments could be due to the solvent-induced fluorescence quenching. Semi-empirical quantum mechanical calculations suggest that μ_e values for 6-AI and 7-AI are better represented by BK′ parameters and polarizability is taken into account, whereas for 5-AI BK parameters explain the value of μ_e with a minor contribution from polarizability.

Acknowledgements

The authors are very grateful to the Department of Science and Technology, New Delhi, for the financial support to project no. SP/SI/H-19/91.

References

[1] J.R. Lakowicz, in Principles of Fluorescence Spectroscopy, Plenum Press, New York, 1982.
[2] J.R. Lakowicz, in Spectroscopy in Biochemistry, CRC Press, Boca Raton, FL, 1981, pp. 195.
[3] J.B. Birks, in Photophysics of Aromatic Molecules, Wiley Interscience, New York, 1970.
[4] C.D. Stubbs, B.W. Williams, in J.R. Lakowicz (ed.), Topics in Fluorescence Spectroscopy; Biochemical Applications, Vol. 3, Plenum Press, New York, 1992, pp. 231.
[5] G.K. Radda, in E.D. Koran (ed.) Methods in Membrane Biology; Biophysical Approach, Vol. 4, Plenum Press, New York, 1975, pp. 97.
[6] P.S. Engel, B.M. Monroe, in G. Hammond, J.N. Pitts (ed.) Advances in Photochemistry, Vol. 8, Academic Press, New York, pp. 245.
[7] C. Reichardt, in Solvents and Solvent Effects in Organic Chemistry, VCH Publishers, Weinheim, Germany, 1988.
[8] A. Kawski, in F. Rabek (ed.), Progress in Photochemistry and Photophysics, Vol. 5, CRC Press, Boca Raton, FL, 1992, pp. 2.
[9] P. Suppan, J. Photochem. Photobiol., A 50 (1990) 293 and references cited therein.
[10] E. Blatt, P. Ghiggino, Biochem. Biophys. Acta 822 (1983) 43 and references listed therein.
[11] S. Mazumdar, R. Manoharan, S.K. Dogra, J. Photochem. Photobiol. A 46 (1989) 301.
[12] R. Manoharan, S.K. Dogra, J. Phys. Chem. 92 (1988) 5282.
[13] J.K. Dey, S.K. Dogra, J. Phys. Chem. 98 (1994) 3638.
[14] A.K. Mishra, M. Swaminathan, S.K. Dogra, J. Photochem. 26 (1984) 49.
[15] M. Swaminathan, S.K. Dogra, J. Am. Chem. Soc. 105 (1985) 6223.
[16] A.K. Mishra, S.K. Dogra, Indian J. Chem. 24A (1985) 285.
[17] P. Phaniraj, A.K. Mishra, S.K. Dogra, Indian J. Chem. 24A (1985) 913.
[18] J.A. Riddick, W.B. Bunger, Techniques in Organic Chemistry—Organic Solvents, Wiley Interscience, New York, 1970.
[19] M. Swaminathan, S.K. Dogra, Indian J. Chem. 22A (1983) 853.
[20] C.A. Parker, Photoluminescence of Solutions with Applications to Photochemistry and Analytical Chemistry, Elsevier, Amsterdam, 1968.
[21] G.G. Guilbault, in Practical Fluorescence, Marcel Dekker, New York, 1971, p. 13.
[22] R.S. Sarpal, S.K. Dogra, J. Chem. Soc. Faraday Trans. I 88 (1992) 2725.
[23] J.C. Tai, N.L. Allinger, J. Am. Chem. Soc. 110 (1988) 2050.
[24] J. Delbene, H.H. Jaffe, J. Chem. Phys. 48 (1968) 1801.
[25] M.J.S. Dewar, E.G. Zoebish, E.F. Healy, J.J. Stewart, J. Am. Chem. Soc. 107 (1985) 3902.
[26] M. Kamiya, Bull. Chem. Soc. Jpn. 43 (1970) 3344.
[27] J.B. Birks, D.J. Dyson, Proc. Roy. Soc. London Ser. A 275 (1963) 135.
[28] S.J. Strickler, R.A. Berg, J. Chem. Phys. 37 (1962) 814.
[29] G. Kohler, J. Photochem. 38 (1987) 217.
[30] M.A. El-Bayoumi, J.M. Dalla, M.F. O'Dwyer, J. Am. Chem. Soc. 92 (1970) 8494.
[31] M. Sow, G. Durocher, J. Photochem. Photobiol. A 59 (1990) 349.
[32] (a) N. Mataga, Bull. Chem. Soc. Jpn. 36 (1963) 654. (b) N. Mataga, T. Kuboto, Molecular Interactions and Electronic Spectra, Marcel Dekker, New York, 1970.
[33] S.R. Meach, D.V. O'Connor, D. Phillips, J. Chem. Soc. Faraday Trans II 79 (1983) 1563.
[34] C. Reichardt, Angew. Chem. Int. Engl. 18 (1979) 98.
[35] D. Goswami, R.S. Sarpal, S.K. Dogra, Bull. Chem. Soc. Jpn. 64 (1991) 3137.
[36] S. Nigam, S.K. Dogra, Indian J. Chem. 32A (1993) 290.
[37] R.A. Loufty, S.M. Walker, Chem. Phys. Lett. 19 (1973) 290.
[38] T.C. Werner, J.H. Sharp, J. Phys. Chem. 83 (1979) 1208.
[39] E.M. Kosower, A. Dodiuk, K. Tanizawa, M. Ottolengni, N. Orbach, J. Am. Chem. Soc. 97 (1975) 2167.
[40] Y. Lic Chen, L. Tyer, R.T. Moody, C.M. Himel, D.M. Hercules, J. Am. Chem. Soc. 97 (1975) 3118.
[41] E.M. Kosower, in An Introduction to Physical Organic Chemistry, Wiley, New York, 1968, pp. 259–384.
[42] E.M. Kosower, J. Am. Chem. Soc. 80 (1958) 3253.
[43] M.J. Kamlet, J.L.M. Abboud, R.W. Taft, Prog. Phys. Org. Chem. 13 (1981) 485 and references listed therein.
[44] M.J. Kamlet, J.L.M. Abboud, M.H. Abraham, R.W. Taft, J. Org. Chem. 48 (1983) 2877.
[45] M.B. Ledger, P. Suppan, Spectrochim Acta. A23 (1967) 3007.
[46] S. Santra, S.K. Dogra, Chem. Phys. 207 (1996) 103.
[47] H. Lumbroso, G. Palamidsessi, Bull. Soc. Chim. Fr. (1965) 3150.
[48] S.K. Saha, S.K. Dogra, J. Lumin., (in press).
[49] Y. Oshika, J. Phys. Chem. Jpn. 9 (1954) 594.
[50] E. Lippert, Z. Naturforsch 10a (1955) 541.
[51] E. Lippert, Z. Naturforsch, Teil A 17 (1962) 621.
[52] N. Mataga, Y. Kaifu, M. Koizumi. Bull. Chem. Soc. Jpn. 28 (1955) 690.
[53] W. Liptay, Z. Naturforsch 20a (1965) 1441.
[54] L. Bilot, A. Kawaski, Z. Elektrochem. 61 (1957) 962.
[55] N.G. Bhakhshiev, Opt. Spektroskopiya 10 (1962) 717.
[56] L.S. Prabhumirashi, D.K. Narayanan Kutty, A.S. Bhide, Spectrochim Acta 19A (1983) 668.